Optical fiber strain sensor using fiber resonator based on frequency comb Vernier spectroscopy

Liang Zhang,[1,2] Ping Lu,[1,2,*] Li Chen,[1,2] Chaoran Huang,[1,2] Deming Liu,[1,2] and Shibin Jiang[3]

[1]*Wuhan National Laboratory for Optoelectronics, School of Optoelectronic Science and Engineering, Huazhong University of Science and Technology, Wuhan 430074, China*

[2]*National Engineering Laboratory for Next Generation Internet Access System (HUST), Wuhan 430074, China*

[3]*AdValue Photonics, 3708 East Columbia Street, Suite 100, Tucson, Arizona 85714, USA*

**Corresponding author: pluriver@mail.hust.edu.cn*

Received January 20, 2012; revised April 9, 2012; accepted April 17, 2012; posted May 4, 2012 (Doc. ID 161618); published June 25, 2012

A novel (to our best knowledge) optical fiber strain sensor using a fiber ring resonator based on frequency comb Vernier spectroscopy is proposed and demonstrated. A passively mode-locked optical fiber laser is employed to generate a phased-locked frequency comb. Strain applied to the optical fiber of the fiber ring resonator can be measured with the transmission spectrum. A good linearity is obtained between displacement and the inverse of wavelength spacing with an R^2 of 0.9989, and high sensitivities better than 40 pm/$\mu\varepsilon$ within the range of 0 to 10 $\mu\varepsilon$ are achieved. The sensitivity can be proportionally improved by increasing the length of the optical fiber ring resonator.

OCIS codes: 060.2370, 300.6360, 140.4050, 140.4780.

Optical fiber strain sensors have been widely used in many fields due to their important advantages including their compact size, electrically passive operation, immunity to electromagnetic interference, high sensitivity, and multiplexing capabilities. Various optical fiber sensing schemes, such as fiber Bragg gratings (FBGs) [1], Mach–Zehnder interferometers, and Michelson interferometers [2], have been developed in strain gauge. FBG sensors have a large measurement range and are widely applied to structural health monitoring. However, their sensitivity of approximately 1 pm/1 $\mu\varepsilon$ challenges the abilities to resolve changes in the order of picometers using small and packaged electro-optics units [1]. Mach–Zehnder and Michelson interferometers have the advantage of high sensitivity, but demonstrate instability and a limited measurement range [2].

Cavity-enhanced direct frequency comb spectroscopy is an advanced technology based on an optical frequency comb efficiently coupled to a high-finesse cavity [3,4], which has been widely used in chemical investigation [5], molecular detection [6,7], medical care [8], and displacement measurements [9,10]. A frequency comb enables the measurement of many characterizations of a broadband high-finesse cavity [11]. The frequency spacing difference between a frequency comb and a resonator can be measured with high resolution by means of frequency comb Vernier spectroscopy [3]. However, the aforementioned techniques are implemented in mirror-based cavities, whose difficult alignment limits their application in strain sensing. Then, a superiorly performed and easily implemented strain sensing system is expected. Therefore, in this Letter, we proposed an alternative scheme for strain sensing using a fiber ring resonator based on frequency comb Vernier spectroscopy, which achieves high sensitivities and is immune to power supply fluctuations. In addition, as an alternative to a mirror-based Fabry–Perot cavity, the fiber ring resonator is low in cost and can be easily fabricated by using a standard telecom fiber.

The schematic configuration of the strain sensor is shown in Fig. 1. A frequency comb generated by a passively mode-locked fiber laser was coupled to a fiber ring resonator. The transmission spectrum was observed with an optical spectrum analyzer (OSA).

Equality in length between the laser cavity and the resonator yields a "magic point" where the comb of the resonator modes and the laser modes are in perfect resonance [10]. In the vicinity of the point, the modes of frequency comb and resonant frequencies of the resonator resemble a Vernier with a Vernier ratio determined by the length ratio [12]. In other words, the transmission spectrum will demonstrate a wavelength spacing, which corresponds to the Vernier ratio and shows that longitudinal modes can travel through the resonator with the highest transmission intensity only when they resonate with both the laser cavity and the resonator. From this it follows such that strain applied to the optical fiber of the resonator changes the wavelength spacing in the transmission spectrum and can be measured with the transmission spectrum.

Every mth mode of the frequency comb can be described as $f_m = mf_{\mathrm{rep}} + f_0$, where f_{rep} is the repetition

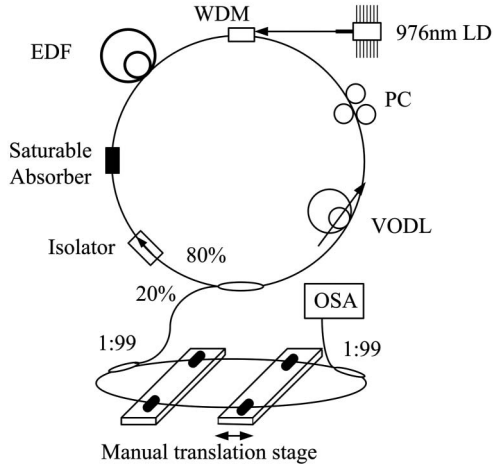

Fig. 1. Schematic of the strain sensor using fiber resonator based on frequency comb Vernier spectroscopy.

rate of the laser, which is relevant to the optical length of the laser cavity, and f_0 is the comb offset frequency (also known as carrier-envelope offset frequency) [3]. The free-spectral range (FSR) of the resonator can be expressed as FSR $= c/nl$, where c is the vacuum speed of light, n is the effective index of fiber, and l is the length of the resonator.

As illustrated in Fig. 2, when FSR$/f_{\text{rep}} = x/(x+1)$ or FSR$/f_{\text{rep}} = x/(x-1)$ is chosen, only every xth comb mode is on resonance [3]. The frequency comb transmitting through the resonator has a frequency spacing of $x \times f_{\text{rep}} = c/n\Delta l$, where Δl denotes the length difference between the laser cavity and the resonator. For sufficiently large x the spacing can be easily resolved with OSA [12]. Assuming that the length of the resonator is larger than that of the laser cavity, the relationship between frequency spacing and strain ($\varepsilon = \Delta l'/l'$) can be described by

$$\frac{1}{x \times f_{\text{rep}}} = \frac{n\Delta l}{c} + \frac{0.78\ \varepsilon n l'}{c}. \tag{1}$$

Furthermore, variance of strain applied to the fiber of the resonator will result in a change in wavelength spacing given by

$$n(0.78\varepsilon l' + \Delta l) = \frac{\lambda_0(\lambda_0 + \Delta\lambda)}{\Delta\lambda}, \tag{2}$$

where $\Delta\lambda$ and λ_0 represent the wavelength spacing and a peak wavelength, respectively, and l' is the length of the fiber to which strain is applied.

In our experimental setup, as shown in Fig. 1, the frequency comb was generated by the passively mode-locked optical fiber laser with a saturable absorber in the form of a fiber taper embedded within a single-wall carbon nanotube polymer composite. A section of erbium-doped fiber (EDF) spliced in the loop was pumped by a fiber-coupled laser diode operating at 976 nm via a 980/1550 nm wavelength division multiplexer (WDM). For optimal operation, an isolator and a polarization controller (PC) were inserted into the loop. The laser output had a linewidth (FWHM) of about 7 nm measured by the OSA. The length of the laser cavity was about 11 m, corresponding to the repetition rate f_{rep} of 18.8 MHz. The

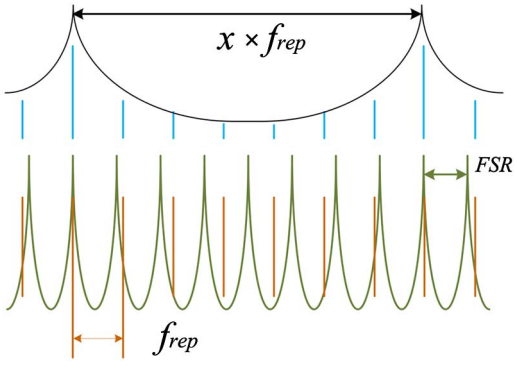

Fig. 2. (Color online) Schematic of frequency comb Vernier spectroscopy. The frequency comb transmitted through the resonator has frequency spacing.

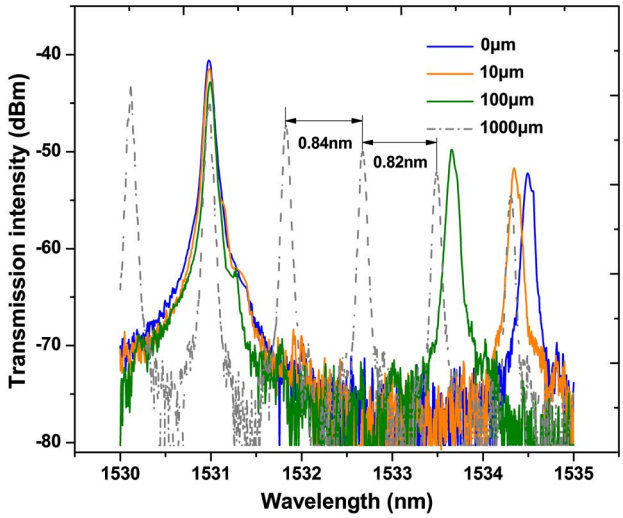

Fig. 3. (Color online) Transmission spectra with displacements of 0, 10, 100, and 1000 μm, respectively.

adjustment of f_{rep} was performed by using a manual variable optical delay line (VODL) inserted in the laser cavity.

The resonator was composed of two single-mode couplers with a coupling ratio of 1:99 and two pieces of single-mode optical fiber. Its round-trip length and round-trip losses were about 11 m and 10.4% (0.48 dB), respectively, giving an FSR of approximately 19 MHz and a finesse of 28 [13]. Two sections of optical fibers of about 5 m as sensing heads were fixed on two manual translation stages using glue.

The tuning range of the VODL (General Photonics VDL-001) is slightly more than 600 ps, which indicates that the length difference between the laser cavity and the resonator should not exceed 12 cm, otherwise the "magic point" will not appear. To obtain high sensitivity, the VODL was slowly tuned till the wavelength spacing was large enough, i.e., 3.5 nm in this experiment. Then, one translation stage was moved by step values of 10 and 100 μm, which corresponded to 2 and 20 $\mu\varepsilon$ for the 5 m fibers, respectively. Figure 3 displays the transmission spectra with displacements 0, 10, 100, and 1000 μm, respectively. The dispersion of the fiber in the resonator results in nonuniformity of the wavelength spacing, as shown in Fig. 3 with displacement of 1000 μm. To reduce its influence on the measurement accuracy, the wavelength spacing was measured when a peak wavelength shifted to a fixed wavelength, i.e., 1531 nm in our experiment. The spacing between the fixed wavelength and the next peak was recorded. The spectrum drift is mainly caused by the fluctuation of the comb offset frequency.

The sensor response, shown in Fig. 4, indicates that the sensor is more sensitive to displacement when the wavelength spacing is larger, which is in good agreement with Eq. (2). Figure 5 shows good linearity between the displacement and the inverse of wavelength spacing ($1/\Delta\lambda$), with an R^2 of 0.9989 and a slope coefficient of about 0.00088, from which we can derive the sensitivity as 8 pm/μm at 50 μm, or 40 pm/$\mu\varepsilon$ at 10 $\mu\varepsilon$. Therefore, the sensitivities within the range of 0 to 10 $\mu\varepsilon$ are better than 40 pm/$\mu\varepsilon$. The slope coefficient is slightly smaller

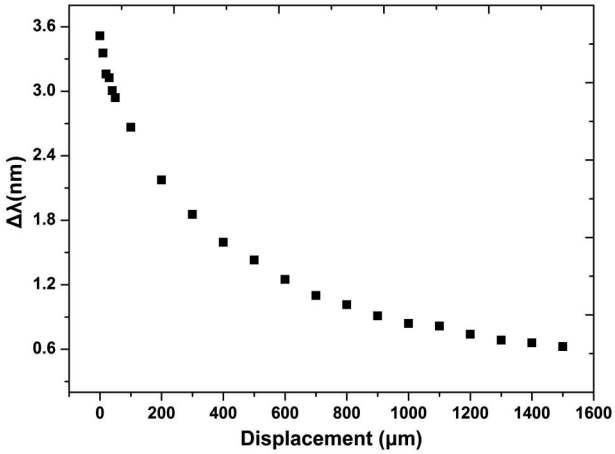

Fig. 4. Response of the sensing head with displacement.

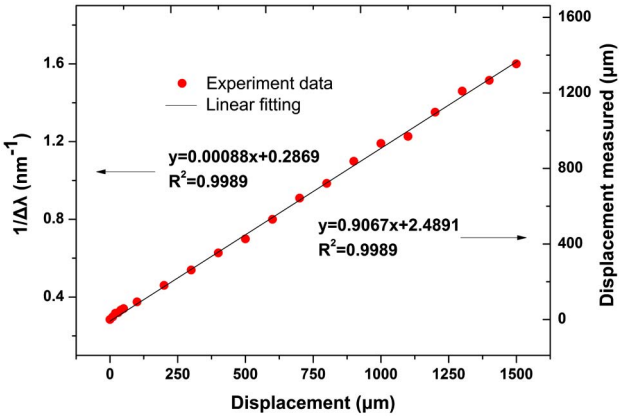

Fig. 5. (Color online) Linear relationship between the displacement and the inverse of wavelength spacing.

than the theoretical value of about 0.00097. Accordingly, the displacements measured are smaller than the displacements of the translation stage, which is probably induced by glue deformation.

The strain sensor achieves high sensitivity enabling its potential applications such as a solid earth tide gauge. Furthermore, according to Eq. (2), increasing the length of the resonator can proportionally improve the detection sensitivity to strain. Some disadvantages of our sensor include its susceptibility to environment and limited gauge range. However, when the sensor works as a solid earth tide gauge, whose working environment is rather stable, temperature disturbance becomes less problematic and the displacement range is small [14].

In summary, we have proposed and experimentally demonstrated a novel (to our best knowledge) optical fiber strain sensor using a fiber ring resonator based on frequency comb Vernier spectroscopy. A frequency comb generated by a passively mode-locked fiber laser was coupled to a fiber ring resonator. The transmission spectrum demonstrates high sensitivities better than 40 pm/$\mu\varepsilon$ within the range of 0 to 10 $\mu\varepsilon$. The sensitivity can be proportionally improved by increasing the length of the optical fiber ring resonator.

This work is supported by a grant (No. 60937002, 60807017) from the Natural Science Foundation of China and a grant (HUST: No. 2011TS058) from the Fundamental Research Funds for the Central Universities. The saturable absorber used in the experiment was provided by Kphotonics, LLC.

References

1. A. D. Kersey, M. A. Davis, H. J. Patrick, M. LeBlanc, K. P. Koo, C. G. Askins, M. A. Putnam, and E. J. Friebele, J. Lightwave Technol. **15**, 1442 (1997).
2. C. K. Kirkendall and A. Dandridge, J. Phys. D **37**, 197 (2004).
3. F. Adler, M. J. Thorpe, K. C. Cossel, and J. Ye, Annu. Rev. Anal. Chem. **3**, 175 (2010).
4. M. J. Thorpe and J. Ye, Appl. Phys. B **91**, 397 (2008).
5. K. C. Cossel, F. Adler, K. A. Bertness, M. J. Thorpe, J. Feng, M. W. Raynor, and J. Ye, Appl. Phys. B **100**, 917 (2010).
6. M. J. Thorpe, K. D. Moll, R. J. Jones, B. Safdi, and J. Ye, Science **311**, 1595 (2006).
7. M. J. Thorpe, F. Adler, K. C. Cossel, M. H. G. de Miranda, and J. Ye, Chem. Phys. Lett. **468**, 1 (2009).
8. M. J. Thorpe, D. Balslev-Clausen, M. S. Kirchner, and J. Ye, Opt. Express **16**, 2387 (2008).
9. Y. Bitou, T. R. Schibli, and K. Minoshima, Opt. Express **14**, 644 (2006).
10. T. Gherman and D. Romanini, Opt. Express **10**, 1033 (2002).
11. A. Schliesser, C. Gohle, T. Udem, and T. W. Hänsch, Opt. Express **14**, 5975 (2006).
12. C. Gohle, B. Stein, A. Schliesser, T. Udem, and T. W. Hänsch, Phys. Rev. Lett. **99**, 263902 (2007).
13. L. F. Stokes, M. Chodorow, and H. J. Shaw, Opt. Lett. **7**, 288 (1982).
14. M. A. Zumberge and F. K. Wyatt, Pure Appl. Geophys. **152**, 221 (1998).